Published in IET Communications
Received on 12th April 2012
Revised on 31st October 2012
Accepted on 24th November 2012
doi: 10.1049/iet-com.2012.0197

ISSN 1751-8628

Two-dimensional spreading scheme employing 2D orthogonal variable spreading factor codes for orthogonal frequency and code division multiplexing systems

Parul Puri, Neetu Singh

Department of Electronics and Communication Engineering, Jaypee Institute of Information Technology, Noida, India
E-mail: parulpuri9@gmail.com

Abstract: Future 4G systems require transmission of richer multimedia services which inevitably implies an increase in data rate. Orthogonal frequency and code division multiplexing (OFCDM) technique has shown promising results in achieving a high data rate while simultaneously combating multipath fading. OFCDM is an amalgamation of orthogonal frequency division multiplexing and two-dimensional (2D) spreading. 2D spreading helps to achieve diversity gains in both time and frequency domains. The present OFCDM systems employ 1D orthogonal variable spreading factor (OVSF) codes to achieve the required 2D spreading in code multiplexed channels. However, 2D OVSF codes have better correlation properties in comparison to 1D OVSF codes. Motivated by this principle, the authors propose a spreading scheme for OFCDM systems using 2D OVSF codes. The spreading scheme is designed to increase the system throughput and reduce multi-code interference. Here, the authors study the OFCDM system performance using the proposed spreading scheme in a multipath fast fading channel with varying spreading factors in both time and frequency domains. The results are compared with the existing OFCDM systems using 1D OVSF codes.

1 Introduction

With the rapid growth of user demands, fourth generation (4G) mobile communication systems are expected to become a platform capable of providing richer multimedia services to the users in comparison to the established 3G systems. This effectively requires an increase in the data rate. High data rate is required for services such as broadcast, thereby making it essential to increase the downlink capacity. 4G systems target a peak data rate of 100 Mbps with a bandwidth of 50–100 MHz in the downlink. Multicarrier modulation techniques are widely being adopted for this purpose. They have shown good results in terms of combating multipath interference.

Orthogonal frequency division multiplexing (OFDM) is one such multicarrier technique [1]. OFDM has shown considerable capabilities in handling multipath interference. OFDM is basically a modulation technique using orthogonal and overlapping sub-carriers to transmit data. The serial data is converted into parallel streams which are transmitted on the orthogonal subcarriers. Furthermore, by opting for appropriate number of subcarriers, OFDM is able to implement fast Fourier transform (FFT), hence, providing a simple modulation–demodulation scheme. In addition, inter symbol interference (ISI) can be easily handled by choosing appropriate size of the guard interval. Several OFDM-based multiple access schemes have been proposed. Namely, OFDM-FDMA, OFDM-TDMA, OFDM-CDMA and OFCDM. OFDM-FDMA and OFDM-TDMA have been adopted by the IEEE 802.16 standard for transmission at the 2.11 GHz band.

Code division multiple access (CDMA) is a multiple access technique based on spread spectrum (SS) signalling [2]. CDMAs several benefits such as anti-jamming, anti-interference, low probability of intercept and accurate universal timing are well known in the art. Furthermore, OFDM-CDMA or multicarrier CDMA has been studied in [3, 4]. In comparison to DS-CDMA, a multi-carrier CDMA system is based on multi-user detection. The system encompasses a receiver that jointly detects all signals to subside the non-orthogonal properties of received signals, hence, it completely utilises the scattered energy of the received signal.

Furthermore, Atarashi *et al.* [5] proposed an Orthogonal Frequency and Code Division Multiplexing (OFCDM) technique. OFCDM can be envisaged as an OFDM system with two-dimensional (2D) spreading in time and frequency domains. Shah *et al.* [6] compare the performance of OFCDM and OFDM systems as an application in 4G systems. Nippon telegraph and telephone (NTT) DoCoMo has built a 4G prototype system using OFCDM which has achieved 5 Gbit/s over a bandwidth of 100 MHz [7, 8].

The developed OFCDM system uses 1D orthogonal variable spreading factor (OVSF) codes. 1D OVSF codes have been widely used to characterise users and user services in the downlink channel by simultaneously

preserving the orthogonality between different channels. However, it has been studied in [9, 10] that 1D spreading sequences do not possess zero cyclic autocorrelation side lobes and cross-correlation functions. Hence, by using an alternative code set the system performance can be increased. Lin *et al.* [11] proposed that 2D spreading sequences can be constructed that have zero cross-correlation properties. One such class of 2D codes is 2D OVSF codes. 2D OVSF codes possess correlation properties that mitigate multipath and multiuser interference.

Here, we study the performance of an OFCDM system using 2D OVSF codes by introducing a 2D spreading scheme. The rest of the paper is organised as follows. Section 2 describes the OFCDM transceiver structure. Section 3 details the used 2D OVSF codes and the proposed 2D spreading scheme. Furthermore, hybrid MMSE with multi code intergenerate (MCI) cancellation technique has been described in Section 4. Section 5 describes the system model used for simulation and discusses the various results obtained. Conclusions and future work are discussed in the last section.

2 OFCDM system

Fig. 1 shows the block diagram of the OFCDM system [12, 13]. It is similar to an OFDM system with the addition of 2D spreading block and code multiplexer. At the transmitter, the information bits are converted from serial-to-parallel into multiple streams equivalent to the number of code channels. Each channel processor then modulates, interleaves and carries out 2D spreading on the data bits. 2D spreading is illustrated diagrammatically in Fig. 2. As shown, the symbol is first spread by a time domain spreading code with spreading factor (SF) = N_T (here $N_T = 4$). This time spread signal is then duplicated on frequency interleaved subcarriers to prevent burst errors. The number of duplicate copies is same as the frequency domain SF = N_F (here $N_F = 2$). The signal obtained after duplication is then multiplied with the frequency domain spreading code. Similarly, 2D spreading is carried out for each symbol. If there are N_C subcarriers being used then at any time instant, $K = N_C/N_F$ symbols can be transmitted at a time on one code channel (Fig. 3). This scheme is replicated for all code channels which are assigned individual time and frequency spreading codes to maintain the orthogonality among each other.

The processed data is then multiplexed at the code multiplexer. In addition to information bits, pilot symbols are also multiplexed for channel estimation. Pilot symbols may be time, frequency or code multiplexed. Code multiplexed scheme provides more flexibility in design [14]. To maintain the orthogonality between pilot and data channels in frequency selective channels, pilot data is spread only in the time domain. The multiplexed data and pilot symbols are then transmitted in parallel on a set of subcarriers. This is realised using an inverse fast fourier transform (IFFT) block. Furthermore, a guard interval is inserted between different symbols to prevent ISI as performed in an OFDM system. Finally, an up conversion is carried out on the parallel to serial converted data and transmitted through the channel.

At the receiver, the guard interval is removed from the down converted signal. Furthermore, an FFT is performed to perform subcarrier down conversion. Channel estimation is carried out using the multiplexed pilot symbols. This is followed by equalisation of received data. The data is then processed by each code channel processor. The processor consists of a despreader, a deinterleaver and a demodulator. Parallel signals from all the code channels are combined to obtain the serial information stream.

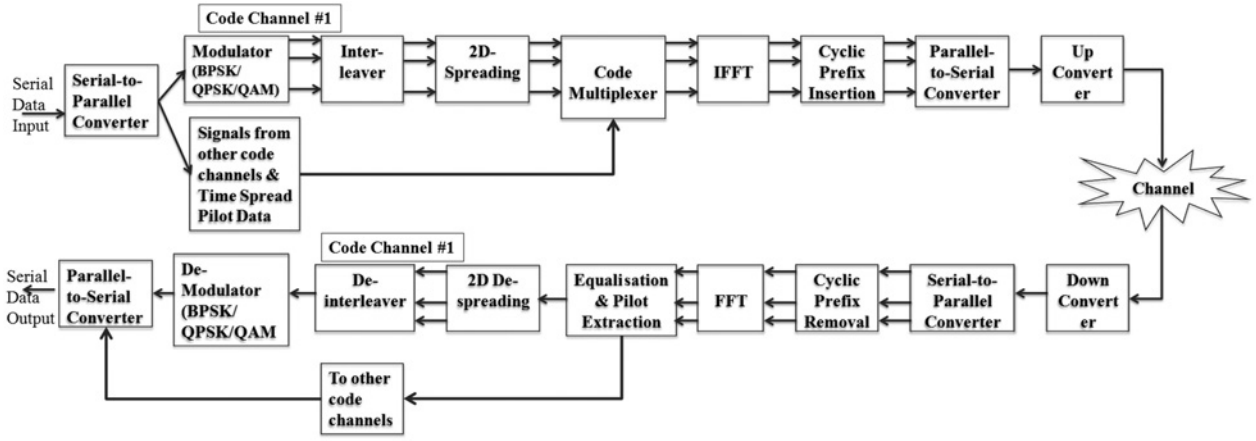

Fig. 1 *OFCDM transceiver structure*

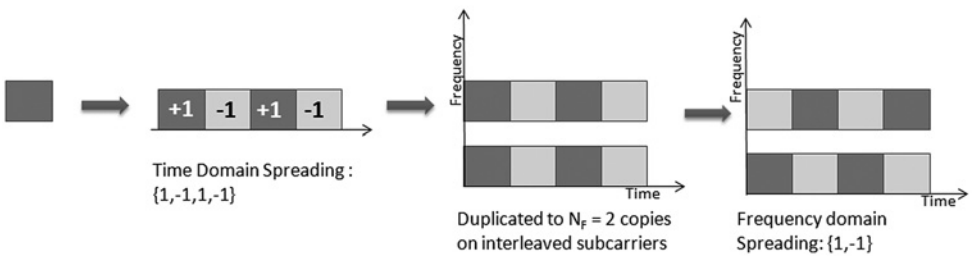

Fig. 2 *2D spreading with 1D OVSF codes [13]*

IET Commun., 2013, Vol. 7, Iss. 5, pp. 463–470
doi: 10.1049/iet-com.2012.0197

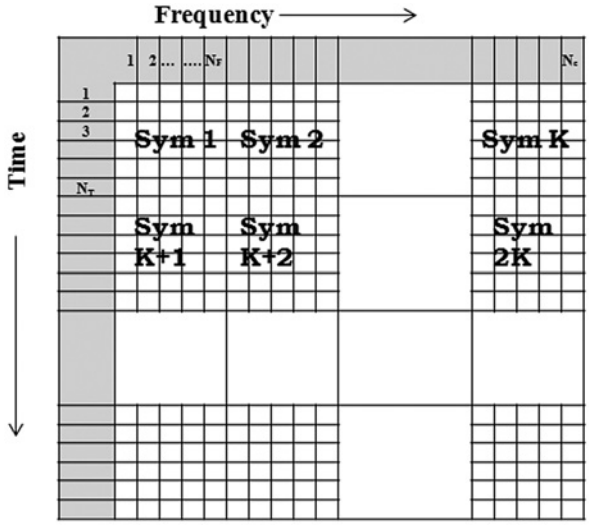

Fig. 3 *Arrangement of 2D spread symbols in time and frequency domains*

3 2D spreading and de-spreading using 2D OVSF codes

Code multiplexing and 2D spreading in the OFCDM system described in Section 2 is achieved by using 1D OVSF codes. 1D OVSF codes and 2D OVSF codes tree structures are shown in Figs. 4 and 5, respectively. The construction of 2D OVSF codes is based on a recursive algorithm [11, 15]. 2D OVSF codes use a seed matrix which represents its first layer. In addition, it uses two 2×2 orthogonal matrices to obtain the second layer. This process is repeated recursively to obtain codes with the required length. The ith layer of 2D OVSF codes consist of 2^i codes of $2^i \times 2^i$ dimension each. We will use the 2D OVSF codes described in [15].

3.1 Spreading

The proposed 2D spreading has been illustrated in Fig. 6. The input data stream is sent over various code channels. Each code channel first modulates the data which is followed by a serial-to-parallel conversion. This gives a $K \times \mathrm{SF}_1$ matrix of modulated data

$\boldsymbol{D}_{\mathrm{ch}} = [\boldsymbol{d}^1_{\mathrm{ch}}, \boldsymbol{d}^2_{\mathrm{ch}}, \ldots, \boldsymbol{d}^K_{\mathrm{ch}}]^{\mathrm{T}}$, where d^k_{ch} is $\mathrm{SF}_1 \times 1$ matrix; $1 \leq \mathrm{ch} \leq \mathrm{Channels}$; $1 \leq k \leq K$.

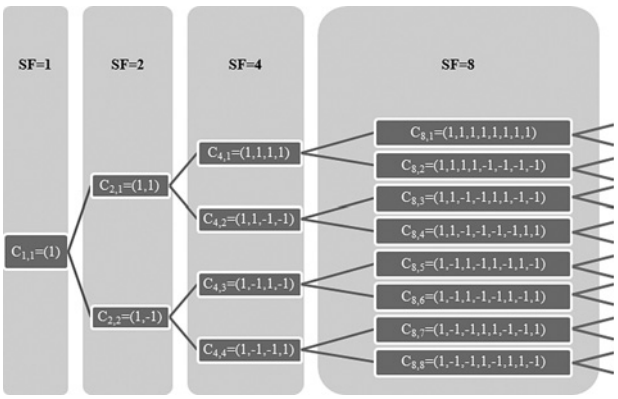

Fig. 4 *1D OVSF codes tree*

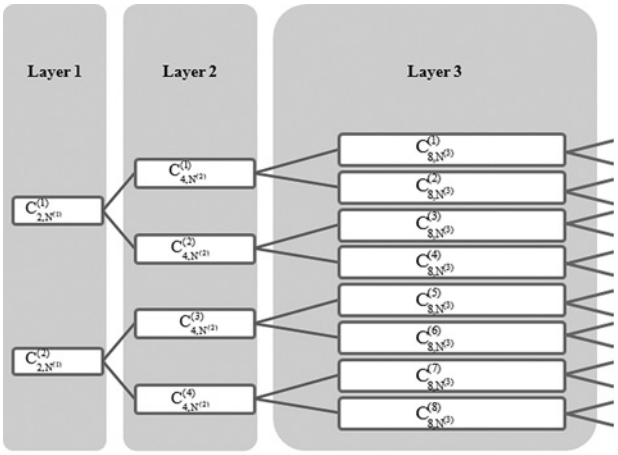

Fig. 5 *2D OVSF codes tree*

Here $K = N_{\mathrm{C}}/N_{\mathrm{F}}$ is the number of parallel streams processed by each channel processor. N_{C} is the number of subcarriers. In each stream, SF_1 bits are simultaneously spread by K different 2D spreaders. The spreading is carried out as follows:

First spreading: SF_1 bits are spread by a 2D OVSF code square matrix of SF_1 dimension, here $N_{\mathrm{T}} = 8$; $N_{\mathrm{F}} = 4$, $\mathrm{SF}_1 = 2$. Such that the 1st bit is spread by first row, 2nd bit by second row and so on till the $(\mathrm{SF}_1)^{\mathrm{th}}$ bit is spread by the last row of the matrix.

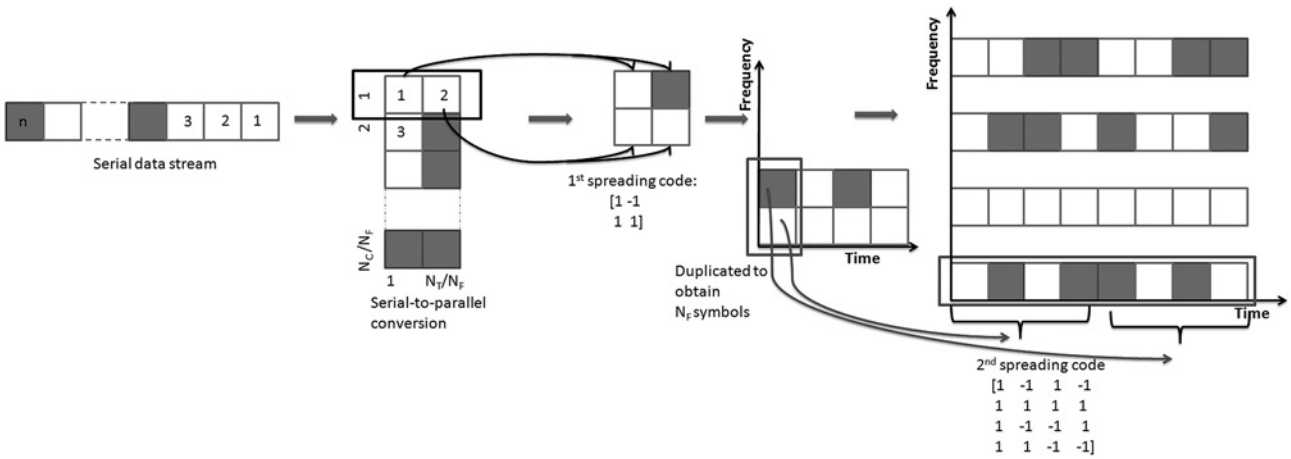

Fig. 6 *2D spreading with 2D OVSF codes*

If $\boldsymbol{C}$ denotes a set of M number of $M \times M$ 2D OVSF code matrices, where M is the SF, and $\boldsymbol{C}^{\text{ch}}_{\text{SF}_1,\text{SF}_1}$ is the spreading matrix of channel ch, then data after 1st spreading are given by a $(\text{K} \times \text{SF}_1) \times \text{SF}_1$ matrix:

$\boldsymbol{T}_{\text{ch}} = [\boldsymbol{t}^1_{\text{ch}}, \boldsymbol{t}^2_{\text{ch}}, \ldots, \boldsymbol{t}^K_{\text{ch}}]$, where $\boldsymbol{t}^k_{\text{ch}}$ is $\text{SF}_1 \times \text{SF}_1$ matrix.

The jth symbol of d^k_{ch} is spread by the jth row of the code matrix as follows

$$\boldsymbol{t}^k_{\text{ch},j} = \boldsymbol{d}^k_{\text{ch},j} * \boldsymbol{C}^{\text{ch}}_{\text{SF}_1,\text{SF}_1};\ \text{where } 1 \le j \le \text{SF}_1$$

Duplication: The obtained matrix is then duplicated in the time domain. This gives a matrix of $(K \times \text{SF}_1) \times N_{\text{F}}$ dimension

$$\boldsymbol{G}_{\text{ch}} = [\boldsymbol{g}^1_{\text{ch}}, \boldsymbol{g}^2_{\text{ch}}, \ldots, \boldsymbol{g}^K_{\text{ch}}];\ \text{where } \boldsymbol{g}^k_{\text{ch}} \text{ is } \text{SF}_1 \times N_{\text{F}} \text{ matrix.}$$

Second spreading: This is carried out by taking the Kronecker tensor product of the duplicated matrix with the frequency domain spreading code matrix of $\text{N}_{\text{F}} \times \text{N}_{\text{F}}$ dimension. Such that the jth symbol is multiplied with the jth row of the code matrix

$\boldsymbol{f}^k_{\text{ch},j} = \boldsymbol{g}^k_{\text{ch},j}$ kron $\boldsymbol{C}^{\text{ch}}_{\text{SF}_2,\text{SF}_{2,j}}$, where $\boldsymbol{f}^k_{\text{ch},j}$ is the Kronecker tensor product of jth symbol of duplicated matrix with dimension $1 \times N_{\text{T}}$. Hence, we obtain an $\boldsymbol{f}^k_{\text{ch}}$ matrix of $N_{\text{F}} \times N_{\text{T}}$ dimension. In all we obtain

$\boldsymbol{F}_{\text{ch}} = [\boldsymbol{f}^1_{\text{ch}}, \boldsymbol{f}^2_{\text{ch}}, \ldots, \boldsymbol{f}^K_{\text{ch}}]$, of $N_{\text{C}} \times N_{\text{T}}$ dimension.

Finally, the signal obtained after code multiplexing from all code channels is as follows:

$\boldsymbol{S} = \boldsymbol{\Sigma}^{\text{Channel}}_{\text{ch}=1} \boldsymbol{F}_{\text{ch}} + \boldsymbol{P}$, where $\boldsymbol{P}$ is the time domain spread pilot data matrix.

It must be noted that this spreading technique is applicable when $N_{\text{T}} > N_{\text{F}}$ and $N_{\text{T}}/N_{\text{F}} > N_{\text{F}}$.

Values of SF_1 and SF_2 are decided as follows:

1. When $N_{\text{T}} \geqq N_{\text{F}}$ and $N_{\text{T}}/N_{\text{F}} \leqq N_{\text{F}}$, $\text{SF}_1 = N_{\text{T}}/N_{\text{F}}$ and $\text{SF}_2 = N_{\text{F}}$
2. When $N_{\text{T}} > N_{\text{F}}$ and $N_{\text{T}}/N_{\text{F}} > N_{\text{F}}$, $\text{SF}_1 = N_{\text{F}}$ and $\text{SF}_2 = N_{\text{T}}/N_{\text{F}}$. Here, the duplication step is eliminated and the Kronecker product is carried out with only the first SF_2 number of rows of second spreading code.
3. When $N_{\text{T}} < N_{\text{F}}$, $\text{SF}_1 = N_{\text{F}}/N_{\text{T}}$, followed by duplication to obtain N_{F} symbols and $\text{SF}_2 = N_{\text{T}}/\text{SF}_1$

3.2 De-spreading

At the receiver, the received data is down converted. Furthermore, the serial data is converted to parallel form

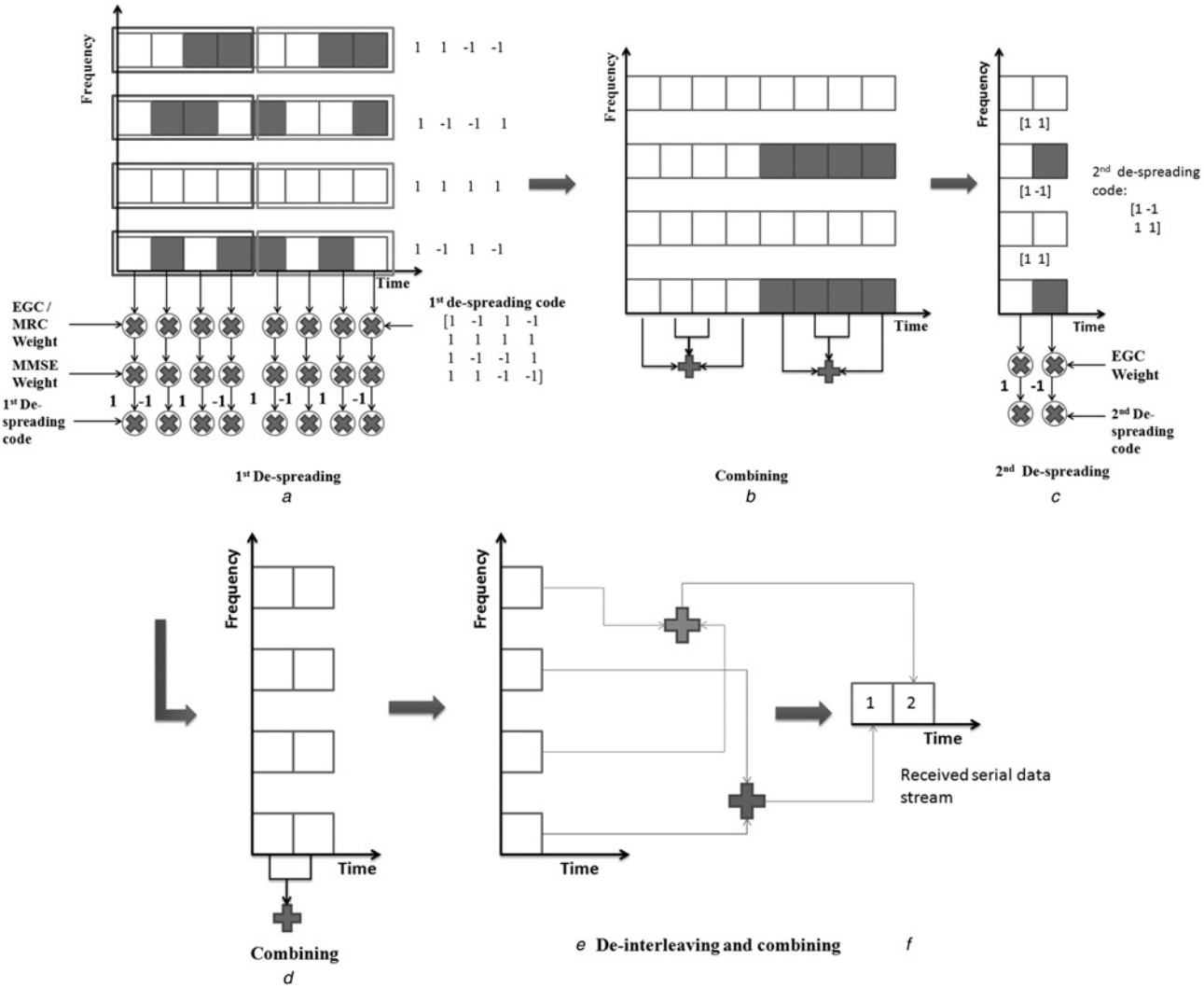

Fig. 7 *2D de-spreading with 2D OVSF codes*

a 1st de-sperading *b* Combining
c 2nd de-sperading *d* Combining
e De-interleaving *f* Combining

doi: 10.1049/iet-com.2012.0197

followed by cyclic prefix removal. This gives a matrix with N_C rows and N_T columns. FFT is performed on this matrix to demodulate the data. The demodulated data needs to be de-spread in accordance with the 2D spreading that was carried out at the transmitter with an aim to remove MCI caused because of code multiplexing of channels. The despreading has been shown in Fig. 7.

In Figs. 7*a* and *b*, first de-spreading is carried out using the code set with $SF = SF_2$. Here, the de-spreader employs either simple equal gain combining (EGC) or maximal ratio combining (MRC) combining to collect spread signals. EGC combining is suitable for modulation techniques such as binary phase shift keying (BPSK) and quadrature phase shift keying (QPSK). However, higher modulation schemes require MRC combining. Figs. 7*c* and *d* shows the second de-spreading. The code set has $SF = SF_1$. Here, the de-spreader employs simple EGC combining to collect spread signals. Finally, the de-spread bits are de-interleaved to obtain a serial data stream. This data stream is de-modulated to obtain the received data.

4 Hybrid detection with MCI cancellation

4.1 Code assignment

As discussed, the proposed spreading scheme uses 2D OVSF codes. Each channel is assigned a set of codes corresponding to their SF values in time and frequency domains, respectively. Hence, the code set for the chth channel can be denoted as $\{\boldsymbol{C}^{ch}_{SF_1}, \boldsymbol{C}^{ch}_{SF_2}\}$. Now, the code sets of the remaining code channels can be divided into two subsets, described as follows:

1. Set A: $\boldsymbol{\omega}_F = \{\boldsymbol{C}^{(ch)}_{SF_1}, \boldsymbol{C}^{(ch')}_{SF_2}\}$, having the same first spreading matrix as the chth code channel, but different second spreading matrix (ch$' \neq$ ch).
2. Set B: $\boldsymbol{\omega}_T = \{\boldsymbol{C}^{(ch)}_{SF_1}, \boldsymbol{C}^{(ch')}_{SF_2}\}$ having a different first spreading matrix to the chth code channel (ch$'' \neq$ ch), but any second spreading matrix (ch$''$ may or may not be equal to ch).

As the codes are orthogonal, there is no interference among the code channels in an additive white Gaussian channel. However, this orthogonality is disturbed because of fast fading in time domain or frequency selective fading in frequency domain. This introduces multi code interference (MCI).

MCI is dependent on the type of codes used [13]. The proposed 2D spreading using 2D OVSF codes helps to reduce MCI. However, in addition to the code set, it is essential to design a code assignment scheme such that MCI is reduced further. Zhou *et al.* [16] have designed a code assignment scheme based on the code distance. The code distance, $d^{(ch,ch')}_{SF_1}$, is given as: $(SF_1/2 + 1 - d_{min})$, where d_{min} is the minimum length of strings of consecutive 1s or −1s in the element wise code product of $\boldsymbol{C}^{(ch)}_{SF_1}.\boldsymbol{C}^{(ch')}_{SF_1}$.

$$\text{where } \boldsymbol{C}^{(ch)}_{SF_1}\boldsymbol{C}^{(ch')}_{SF_1} = \{\boldsymbol{c}^{(ch)}_{SF_1}\boldsymbol{c}^{(ch)}_{SF_{1,0}}, \ldots, \boldsymbol{c}^{(ch)}_{SF_1,SF_1-1}\boldsymbol{c}^{(ch)}_{SF_1,SF_1-1}\}$$

It is preferred to assign codes with greater code distances among adjacent code channels. The non-sequential code assignment scheme and 2D OVSF codes based 2D despreading have significantly reduced MCI in systems using BPSK and QPSK modulation schemes. However, it is observed in higher modulation schemes, such as *M*-ary QAM that the techniques are not sufficient. Hence, it is essential to further reduce MCI.

Zhou *et al.* [17] have proposed a hybrid detection scheme for MCI removal based on the following assumption. Since, high speed data transmission is required the packet duration is very small (nearly 0.5 ms). Thus, the channel variation is neglected in one packet duration. Therefore orthogonality among channels is preserved because of time domain spreading. However, as the channel is frequency selective, the orthogonality between code channels in frequency domain is distorted. This causes MCI and needs to be cancelled.

As explained, Zhou *et al.* [17] have focused more towards removal of MCI caused because of loss of orthogonality in frequency domain. It is assumed that time domain orthogonality is maintained. However, we know the channel is unpredictable. With increasing time domain spreading factor, the orthogonality relies on the orthogonality of time domain spreading codes. In this case, orthogonality is more sensitive to time-variant properties of the channel and less to frequency-selective fading. Hence, it is equally important to tackle MCI in time domain also. Thus, here we study the effects of MCI in both the domains.

4.2 Proposed hybrid detection with MCI-cancellation in time and frequency domains

The block diagram of the hybrid detection scheme is shown in Fig. 8. After obtaining the demodulated serial data stream

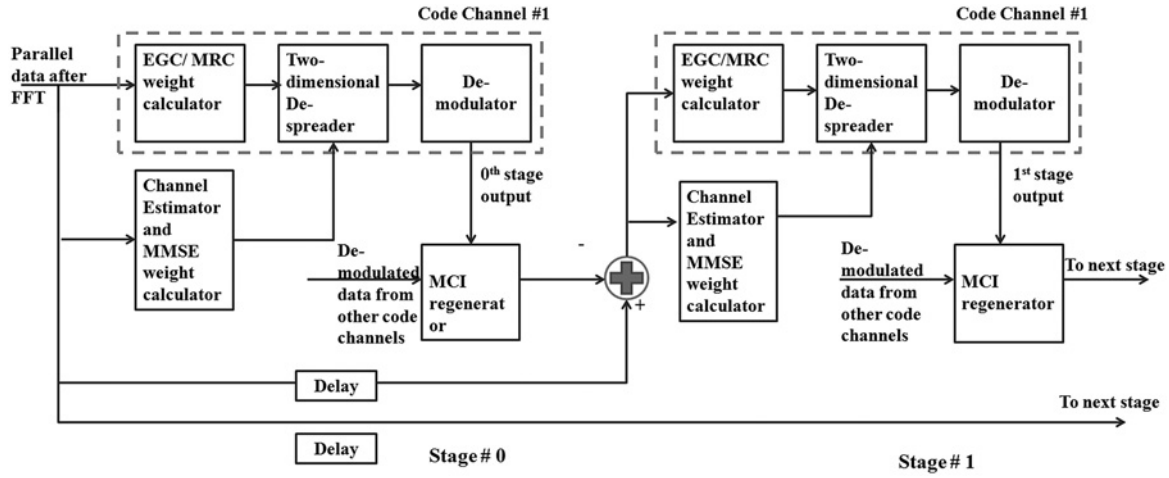

Fig. 8 *Block diagram of hybrid MCI cancellation with MMSE detection*

from Stage # 0 MCI for the subsequent stage is calculated using the following steps:

Data replication: The demodulated serial data is converted to parallel streams for processing. Each channel processor uses its individual 2D spreader to spread the data in both time and frequency domains. This spreading is similar to the one carried out at the transmitter.
MCI calculation: For the chth code channel, MCI is caused by the remaining data channels. Hence, the recovered information bits from other data channels are used to regenerate the MCI for the current data channel (ch). In addition, using the known pilots and channel estimation data, MCI because of pilots is calculated.
MMSE weight calculation: The weights of MMSE are derived and updated stage by stage of MCI cancellation. Total MCI because of data channels is subtracted from the FFT matrix and updated MMSE weights are calculated from this matrix.
MCI cancellation: The calculated MCI because of pilot channel and remaining code channels is subtracted from the FFT matrix to give the MCI removed matrix for the current code channel. The MCI removed matrix is then de-spread and demodulated using the updated MMSE weights. This cancellation process is continued in an iterative way until a specified number of stages are reached or optimum results are achieved.

In general, as the recovered information bits become more reliable with every stage the MCI can be regenerated with higher accuracy stage by stage. After subtraction, a significant amount of MCI can be cancelled out from the received signal. Thus the bit-error-rate (BER) performance can be improved stage by stage.

5 Results and analysis

Figs. 9–13 show the obtained computer simulated results. Fig. 9 compares the performance of the OFCDM system using 1D OVSF codes against OFCDM system using 2D OVSF codes for achieving 2D spreading. The results are obtained by keeping a fixed SF = $N_T \times N_F$, where $N_T = 8$, $N_F = 4$. One code channel is assigned for pilot data while the rest $(N_T - 1) \times N_F$ channels are fully loaded with information bits. As can be seen, the proposed system gives improved results with respect to the OFCDM system

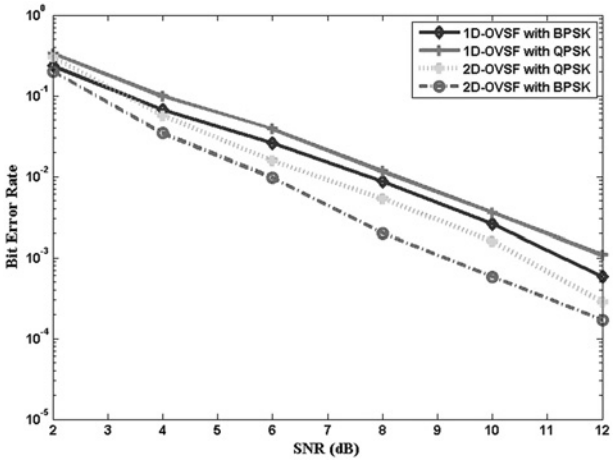

Fig. 9 *System performance curves using 1D OVSF and 2D OVSF codes with BPSK and QPSK modulation schemes and SF = 8 × 4*

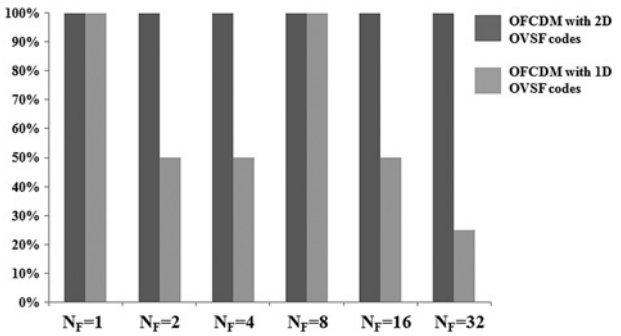

Fig. 10 *Relative throughput with $N_T = 8$ constant, and varying N_F from 1, 2, 4, 8, 16 and 32*

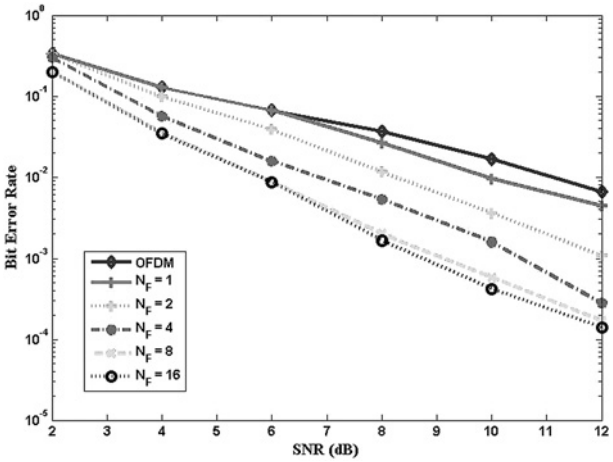

Fig. 11 *System performance curves keeping $N_T = 8$ constant, and varying N_F from 1, 2, 4, 8 and 16 with QPSK modulation*

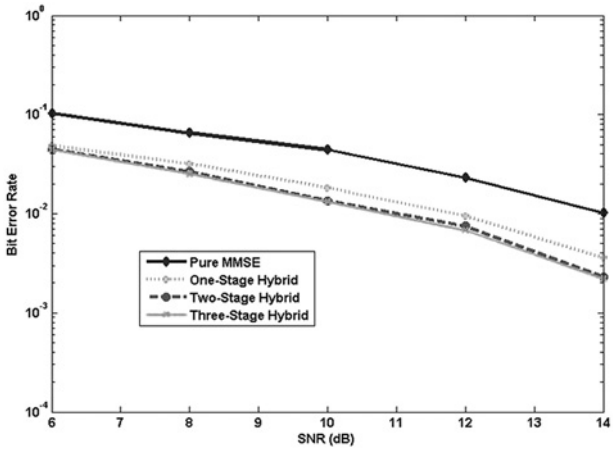

Fig. 12 *OFCDM system performance employing 2D OVSF codes with 8-QAM modulation using hybrid detector $N_T = 8$, $N_F = 4$*

employing 1D OVSF codes. A 2 dB gain in SNR is observed at a BER of 10^{-3} with QPSK modulation.

In addition, the OFCDM – 2D – OVSF scheme has a higher throughput in comparison to OFCDM – 1D – OVSF scheme. This can be inferred by calculating the number of bits processed in the same time period for both the schemes. Taking the following parameters: $N_C = 1024$; $N_T = 8$; $N_F = 4$; code channels (ch) = $N_T \times N_F = 32$; pilot

doi: 10.1049/iet-com.2012.0197

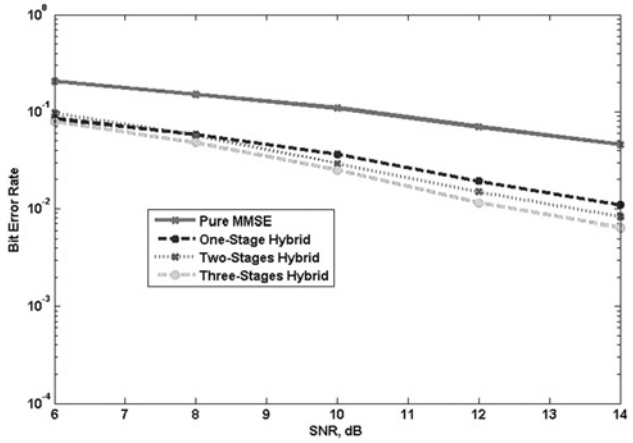

Fig. 13 *OFCDM system performance employing 2D OVSF codes with 16-QAM modulation using hybrid detector $N_T = 8$, $N_F = 4$*

channel = 1; data channels (ch − 1) = 31; modulation scheme (m) = QPSK

OFCDM–1D OVSF scheme: Each code channel processes N_C/N_F bits in parallel. Hence, $(N_C/N_F \times (\text{ch} - 1) \times m) = (1024/4 \times 31 \times 2) = 15872$ bits are processed simultaneously.

OFCDM–2D OVSF scheme: In addition to N_C/N_F bits, additional bits are processed by each code channel depending on the N_T and N_F values. The additional bits are equivalent to the SF_1 value as given below:

1. When $N_T \geqq N_F$ and $N_T/N_F \leqq N_F$, $SF_1 = N_T/N_F$.
2. When $N_T > N_F$ and $N_T/N_F > N_F$, $SF_1 = N_F$.
3. When $N_T < N_F$, $SF_1 = N_F/N_T$.

SF_1 values for $N_T = 8$ and varying N_F are tabulated in Table 2.

For the given parameters, additional bits are $SF_1 = N_T/N_F = 2$. Hence, $(N_C/N_F \times (\text{ch} - 1) \times m \times SF_1) = (1024/4 \times 31 \times 2 \times 2) = 31744$ bits are processed simultaneously. This clearly indicates that the choice of time and frequency domain SF varies the system throughput in the proposed system.

Table 1 System parameters

Parameter	Value
environment	single-cell
channel	2-Tap Rayleigh fading channel (SUI-5 Model)
bandwidth	100 MHz
subcarriers	1024
code assignment	non-sequential
pilot structure	code multiplexed
estimation	MMSE/MMSE with MCI cancellation
modulation	BPSK/QPSK/8-QAM/16-QAM
codes	1D OVSF/2D OVSF
diversity scheme	EGC/MRC

Table 2 N_F and SF_1 values with $N_T = 8$

N_F	1	2	4	8	16	32
SF_1	1	2	2	1	2	4

Fig. 10 shows the relative throughputs of the two systems, that is, OFCDM using 1D OVSF codes for spreading against OFCDM using 2D OVSF codes. N_T is kept constant (= 8) and N_F is varied. The total number of code channels is kept equal to the $SF = N_T \times N_F$. This helps to achieve the same data rate as an OFDM system. As can be seen from Fig. 10, the relative throughput of the OFCDM–2D OVSF system is greater than that of the OFCDM–1D OVSF system for certain values of spreading factors. For $N_F = 2$, 4 and 16 and $N_T = 8$, OFCDM–2D OVSF has double throughput. This increase in throughput is irrespective of the chosen modulation scheme.

Fig. 11 shows the performance curves by keeping $N_T = 8$ constant, and varying N_F from 1, 2, 4, 8. Varying N_F is helpful in studying the multipath propagation effects of the channel. When $N_F = 1$, there is not much improvement in the performance as compared with an OFDM system for lower SNR values. However, beyond that there is a significant increase in performance with increasing SNR. A gain of 5 dB in SNR at a BER of 5×10^{-3} is achieved as we increase N_F from 1 to 16. This is mainly because of the increase in frequency diversity gain with increased spreading in frequency domain. Frequency domain spreading is basically the duplication of time spread data on multiple carriers by using suitable codes. Hence, this increases the frequency diversity gain. However, it is observed that beyond $N_F = 8$, the performance becomes stable and does not improve further. It is due to the increase in MCI as the frequency domain spreading factor is increased. This problem can be overcome by employing hybrid detection with MCI cancellation.

Figs. 12 and 13 show the BER plots of the OFCDM system using 2D OVSF codes with MMSE detection employing the hybrid MCI cancellation scheme. Fig. 12 shows the results for the 8-QAM modulation scheme. In case of good channel estimation, the hybrid MCI cancellation scheme can be built upon it to mitigate MCI and decrease BER of the system. Furthermore, as seen from Fig. 12, the system performance saturates after the second stage. No further improvement can be achieved using more number of stages in the hybrid detection scheme.

Fig. 13 shows a similar comparison using the 16-QAM modulation scheme. At a BER of 10^{-2}, SNR gain of 3 dB is achieved as we move from the 0th stage to the 3rd stage of hybrid detection. Comparing Figs. 12 and 13 it is seen, that the error has increased with increase in modulation scheme. Furthermore, the system performance saturates after the third stage for 16-QAM. Hence, higher the modulation scheme more number of stages of hybrid detection are required. This increases system complexity.

6 Conclusion

An OFCDM system with 2D OVSF codes-based spreading and hybrid detection was successfully implemented. The system performance was tested and compared with previous OFCDM systems using 1D OVSF codes. As anticipated, because of the better correlation properties of the 2D OVSF codes in comparison with 1D OVSF codes, an improvement in system performance of OFCDM with 2D OVSF codes is observed. In addition, the proposed 2D spreading scheme also helps to increase the overall throughput depending on the chosen spreading factor ratio. Hence, overall a decrease in BER and increase in throughput have been achieved. Furthermore, hybrid MMSE with MCI cancellation

technique proved to be beneficial for detection at receiver for higher modulation schemes. However, it was observed, saturation is reached after a certain number of stages in the hybrid detector. This is due to the limitation of the modulation technique employed. As a part of the future work, more classes of orthogonal code sets can be exploited for achieving further reduction in MCI.

7 References

1 Prasad, R.: 'Wireless communications systems' (Artech House, 2004)
2 Pickholtz, R., Schilling, D., Milstein, L.: 'Theory of spread spectrum communications – a tutorial', *IEEE Trans. Commun.*, 1982, **30**, (5), pp. 855–884
3 Hara, S., Prasad, R.: 'Overview of multicarrier CDMA', *IEEE Commun. Mag.*, 1997, **35**, (12), pp. 126–133
4 Fazel, K., Kaiser, S.: 'Multi-carrier and spread spectrum systems' (John Wiley and Sons, 2003)
5 Atarashi, H., Abeta, S., Sawahashi, M.: 'Variable spreading factor orthogonal frequency and code division multiplexing (VSF-OFCDM) for broadband packet wireless access', *IEICE Trans. Commun.*, 2003, **E86-B**, (1), pp. 291–299
6 Shah, S.M., Umrani, A.W., Memon, A.A.: 'Performance comparison of OFDM, MC-CDMA and OFCDM for 4G wireless broadband access and beyond'. Proc. PIERS, Marrakesh, Morocco, March 2011, pp. 1396–1399
7 Atarashi, H., Abeta, S., Sawahashi, M.: 'Broadband packet wireless access appropriate for high-speed and high-capacity throughput'. Proc. IEEE VTC'01-Spring, May 2001, pp. 566–70
8 Kishiyama, Y., Maeda, N., Higuchi, K., Atarashi, H., Sawahashi, M.: 'Transmission performance analysis of VSF-OFCDM broadband packet wireless access based on field experiments in 100-MHz forward link'. Proc. IEEE VTC'04-Fall, September 2004, **5**, pp. 3328–3333
9 Tseng, S.H., Bell, M.R.: 'Asynchronous multicarrier DSCDMA using mutually orthogonal complementary sets of sequences', *IEEE Trans. Commun.*, 2000, **48**, (1), pp. 53–59
10 Chen, H.H., Yeh, J.F., Suehiro, N.: 'A multicarrier CDMA architecture based on orthogonal complementary codes for new generations of wideband wireless communications', *IEEE Commun. Mag.*, 2001, **39**, (10), pp. 126–135
11 Lin, C.L., Lee, P.J., Chang, C.Y., Yang, G.C., Kwong, W.C.: 'A new frequency-time-spreading code for MC/DS-CDMA wireless systems over Rayleigh fading channels'. Proc. IEEE Sarnoff Symp., May 2007, pp. 1–5
12 Zhou, Y., Wang, J., Ng, T.-S.: 'Two dimensionally spread OFCDM systems for 4G mobile communications'. Proc. IEEE Tencon, October 2007, pp. 1–4
13 Zhou, Y., Ng, T.-S., Wang, J., Higuchi, K., Sawahashi, M.: 'OFCDM: a promising broadband wireless access technique', *IEEE Commun. Mag.*, 2008, **46**, (3), pp. 38–49
14 Kishiyama, Y., Maeda, N., Atarashi, H., Sawahashi, M.: 'Investigation of optimum pilot channel structure for VSF-OFCDM broadband wireless access in forward link'. Proc. VTC, 2003, pp. 139–44
15 Wu, D., Spasojevic, P., Seskar, I.: 'Two-dimensional orthogonal variable-spreading-factor codes for multichannel DS-UWB'. Proc. 38th Asilomar Conf. on Signals, Systems and Computers, December 2004, pp. 627–631
16 Zhou, Y.Q., Wang, J., Ng, T.-S.: 'A novel code assignment scheme for broadband OFCDM systems'. Proc. IEEE Tencon, 2006, pp. 1–4
17 Zhou, Y.Q., Wang, J., Sawahashi, M.: 'Downlink transmission of broadband OFCDM systems – Part I: hybrid detection', *IEEE Trans. Commun.*, 2005, **53**, pp. 718–29

doi: 10.1049/iet-com.2012.0197